

Spatial Variations of Particulate Matter in Mid-West Jordan

Enas M. Al-Hourani^{a,b}, Shatha Suleiman Ali-Saleh^c, Mohammad A. Majali^d, Omar Al-Jagheer^e, Abdulrahman M. Shniekat^a, Mohammad A. Al-Qenneh^a and Tareq Hussein^{a,e}

^a The University of Jordan, School of Science, Department of Physics, Environmental and Atmospheric Research Laboratory (EARL), Amman 11942, Jordan.

^b Mu'tah University, College of Science, Department of Physics, Karak 61710, Jordan.

^c National University College of Technology, Department of Basic Sciences, Amman 11191, Jordan.

^d The Ministry of Education, Directorate of Education for the Karak Region, Karak, Jordan.

^e University of Helsinki, Faculty of Science, Institute for Atmospheric and Earth System Research (INAR), PL 64, FI-00014 UHEL, Helsinki, Finland.

Doi: <https://doi.org/10.47011/17.4.5>

Received on: 06/02/2023;

Accepted on: 27/03/2023

Abstract: We evaluated aerosol concentrations in the northwestern region of Jordan (Amman, Salt, Madaba, Tafila, and Karak) using a simple mobile aerosol measurement setup during April 2022. The submicron particle number (PN₁) concentration was highest in Amman ($4.6 \times 10^4 \text{ m}^{-3}$) and lowest in Karak ($2.0 \times 10^4 \text{ cm}^{-3}$). The main roads connecting these cities exhibited PN₁ between $1.5 \times 10^4 \text{ cm}^{-3}$ and $6.6 \times 10^3 \text{ cm}^{-3}$. The mean micron particle number (PM₁₀₋₁) concentration varied between 2 cm^{-3} and 5 cm^{-3} on roads and from 3 cm^{-3} to 5 cm^{-3} in cities. Micron particulate mass (PM₁₀₋₁) concentrations were higher in cities than on main roads, except for Amman-to-Karak road through Madaba, ($\sim 128 \mu\text{g m}^{-3}$). Amman had the lowest PM₁₀₋₁ concentrations ($\sim 34 \mu\text{g m}^{-3}$). The average concentrations of PM_{2.5} decreased as we moved southward from Amman. The outcomes of this study suggest that traffic emissions are the main sources of aerosols in cities. The southernmost locations (i.e. Karak) were mainly affected by dust aerosols due to local sand re-suspension from desert areas. As a recommendation, long-term aerosol measurements at multiple sites throughout the country, along with more extensive and repeated mobile measurements, are needed.

Keywords: Particle size distributions, Dust storms, Aerosol, Submicron particle, Particle mass.

1. Introduction

The climate impacts of aerosols can be realized in two ways: direct and indirect impacts. For example, aerosol particles are capable of absorbing and scattering solar radiation causing direct effects on the Earth's radiation balance. While aerosols reflect short-wavelength radiation back into space, which cools the Earth's atmosphere, they can also absorb long-wave terrestrial radiation. Aerosol particles can also

affect the climate indirectly by forming cloud droplets. These droplets are formed in the troposphere by condensation of water vapor onto aerosol particles, cloud condensation nuclei, or what is called ice nuclei (CCN or IN) [1]. Besides the effects on the climate, aerosols also cause loss of visibility in urban areas.

In many Arab countries, environmental problems related to air pollution have not received sufficient scientific attention. Although monitoring stations in some Arab countries have been operating for more than two decades, active discussion and reporting of air pollution have lagged behind other regions of the world. Existing studies focus primarily on particulate matter, airborne dust (monitoring, source region, and transport), aerosol optical properties, chemical analysis, and gaseous pollution [2–16]. Very few studies focused on the measurement of size distributions and particle number concentrations [8, 13, 17, 18]. Recently advancements in aerosol measurement technology, particularly for particle size distribution of the particulate matter have gained importance within atmospheric science. Consequently, measuring particle number and mass size distributions has become a major research focus at the Environmental and Atmospheric Research Laboratory (EARL, University of Jordan) in Jordan [8–13, 19–22]. Besides our own research conducted at the EARL, only a few studies on air pollution in Jordan exist [23–26].

Urban aerosol measurements are important to establish proper linkages between air pollution and its harmful impacts on human health. Such measurements are also needed to assess the effectiveness of air quality regulations. Quantifying the particle size distributions (PSDs) of urban aerosols is essential to understanding the size-dependent mechanisms that regulate particle transport, transformation, and fate in the urban atmosphere [27].

This paper is a continuation of our efforts to measure and report particulate matter concentrations in Jordan, expanding coverage to the mid-western region (including Amman, Salt, Madaba, Tafila, and Karak). The experimental setup was based on a mobile arrangement of portable instruments that are capable of measuring the particulate matter concentrations across various particle size fractions and metrics (both number and mass concentrations in several size fractions from 0.01 to 25 μm in particle diameter). This study provided important preliminary information about particulate matter

concentrations over a large geographic area in Jordan while accounting for diverse particle size fractions in the atmosphere of these governorates, with high accuracy regarding sampling time and location.

2. Materials and Methods

2.1. Description of the Measurement Campaign

The measurement campaign took place during April 10 – 28, 2022. During this period, we conducted three rounds of measurements in different governorates. We used portable instruments in a mobile setup to measure aerosol concentrations (number and mass) across several cities and along major routes in Jordan (Fig. 1).

First track (April 10): We started driving around 9:00 am from Amman (University of Jordan) and then headed west to Salt, where we made a full tour around Salt city before returning to Amman. The tour took 4 hours and the distance traveled was about 45 km.

Second track (April 12): Starting at around 10:00 am from Amman (University of Jordan), we headed south along the desert road to Karak Governorate, then turned west towards the Jordan Valley (Ghor Al Mazraa), the lowest point on Earth at 420 m below sea level. After that, we headed south along the Dead Sea until we reached Ghor Al Safi and Ghor Al Fifa. Then we headed east to Tafila Governorate, passing through the main street in Tafila City. After that, we headed north to Karak Governorate, where measurements were made in several areas of Karak Governorate, including the city of Karak, after which the tour ended. This route spanned about 317 km and lasted 8 hours.

Third track (April 28): We started driving at around 8:30 AM from Amman (University of Jordan) then headed southwest to Madaba Governorate, continuing southward to Madaba city and on to Dheban, passing Al Wala. Then we went to Karak Governorate passing Mujib Dam, where we made several measurements across the northern and central parts of the Karak Governorate. The tour took 8 hours, and the approximate distance traveled on this track was about 237 km.

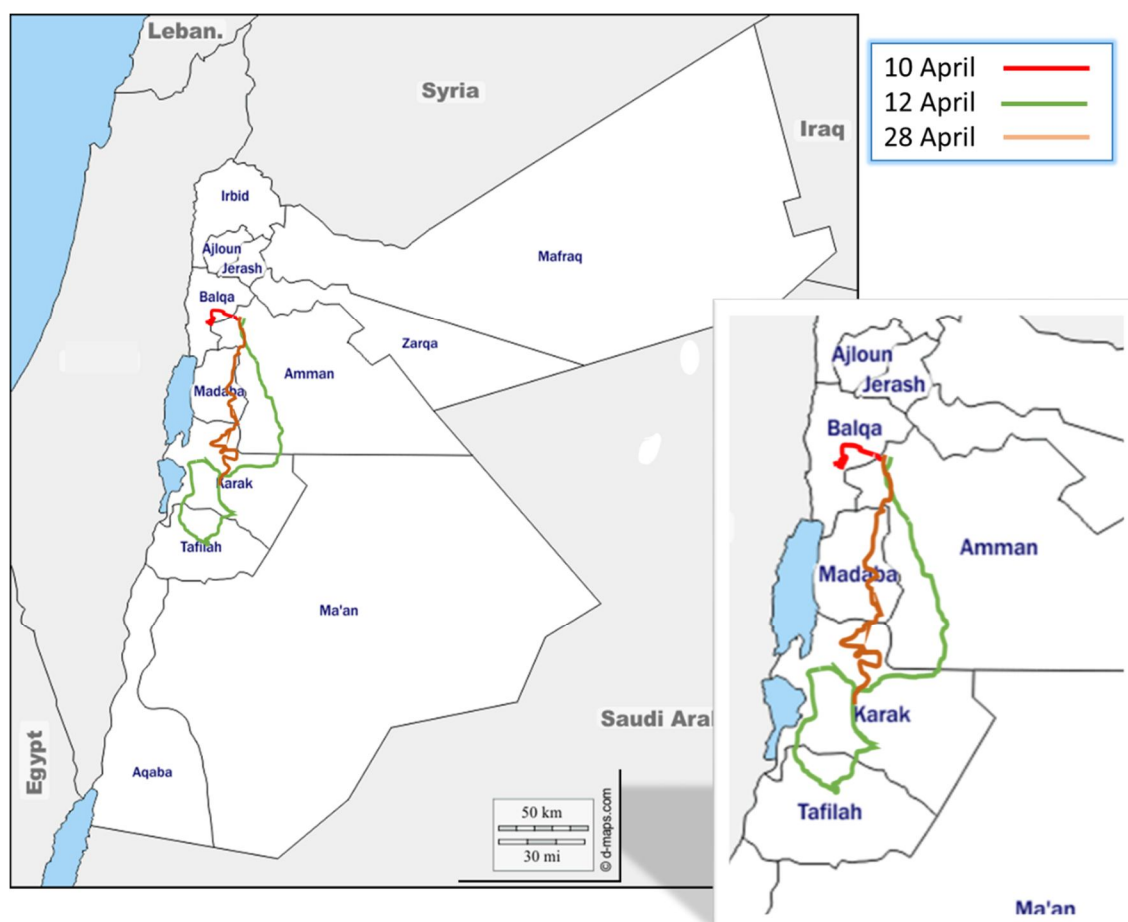


FIG. 1. Map of Jordan that shows the driving routes.

2.2. Mobile Experimental Setup

The mobile experimental setup included three portable instruments: two condensation particle counters (TSI CPC 3007-2 and P-Trak 8525) and a handheld optical particle counter (TSI AeroTrak 9306-V2).

The CPC and the P-Trak have cutoff particle diameters of 10 and 25 nm, respectively, and measure total sub-micron particle number concentrations up to a couple of microns in diameter. The maximum detectable concentrations for these counters are 10^5 cm^{-3} and $50 \times 10^4 \text{ cm}^{-3}$ (20% accuracy), respectively. The sampling flow rate was 0.1 L min^{-1} (inlet flow rate 0.7 L min^{-1}) in both counters.

The AeroTrak was used to measure size-specific particle number concentrations within an optical diameter range of 0.3–25 μm across six channels: 0.3–0.5, 0.5–1, 1–2.5, 2.5–5, 5–10, and 10–25 μm . The sampling time resolution was 1 s at a flow rate of 2.83 L min^{-1} .

Portable low-cost sensors (LCS, Panasonic assembled in-house by Nagoya University) were included in the mobile setup to measure particulate matter ($\text{PM}_{2.5}$) as a complementary setup alongside the portable counters. These LCS also recorded relative humidity (RH) and temperature (T) during the measurement.

We used a Garmin GPS (eTrex 32x) to record the speed and location of the mobile laboratory with a 1-second time resolution.

All instruments were situated on the back seat of a car (Jeep Cherokee, 2013). While driving, we kept the front windows and the back windows fully open. This guaranteed a high exchange rate between indoor and outdoor air, providing representative outdoor aerosol measurements. We, therefore, did not need special inlets for the aerosol instruments in this simple “mobile setup”. Before each measurement session, we checked all devices for readiness and synchronized the instrument clocks.

2.3. Aerosol Data Handling

The raw data underwent a quality check and was then converted to a one-minute average database. We also calculated average concentrations during different periods: (1) periods spent crossing each city and (2) periods spent on the main roads between cities. In total, we visited five cities: Amman, Salt, Madaba, Tafila, and Karak. As for the main roads between cities, we traveled along nine roads: Amman–Salt, Amman–Madaba, Desert (between Amman and Qatrana), Qatrana–Karak, Madaba–Karak, Karak–Ghor, Jordan Valley (Dead Sea), Dead Sea (industrial area)–Tafila, and Tafila–Karak.

We obtained particle number concentrations (PN) in eight particle size fractions within the following diameter ranges: 10–25 nm (calculated from the difference between the concentrations measured with the CPC and the P-Trak), 25–300 nm (calculated from the difference between the concentrations measured with the P-Trak and the AeroTrak), 0.3–0.5 μm , 0.5–1 μm , 1–2.5 μm , 2.5–5 μm , 5–10 μm , and 10–25 μm . The last six particle size channels were measured directly with the AeroTrak.

The normalized particle number size distribution (n_N^0) was calculated by normalizing the particle number concentration (PN) in each size fraction to its corresponding particle diameter range:

$$n_N^0 = \frac{dN}{d\log(D_p)} = \frac{N}{\log_{10}(D_{p2}) - \log_{10}(D_{p1})} \quad (1)$$

where N is the size-specific particle number concentration and D_{p1} and D_{p2} are, respectively, the lower and upper particle diameter limits of that corresponding particle size-fraction.

The normalized particle mass size distribution (n_M^0) was calculated by assuming spherical particles with unit density:

$$n_M^0 = \frac{dM}{d\log(D_p)} = \frac{\frac{\pi}{6}\langle D_p \rangle^3 \rho_p N}{\log_{10}(D_{p2}) - \log_{10}(D_{p1})} = \frac{\pi}{6} \langle D_p \rangle^3 \rho_p n_N^0 \quad (2)$$

where $\langle D_p \rangle$ is the mean particle diameter of the particle size channel, ρ_p is the particle bulk density, and N is the size-specific particle number concentration, with D_{p1} and D_{p2} as diameter limits.

The particle number (PN) or mass (PM) concentration in any particle size fraction can be calculated by integration:

$$PN = \int_{D_{p1}}^{D_{p2}} n_N^0 d\log(D_p) \quad (3)$$

$$PM = \int_{D_{p1}}^{D_{p2}} n_M^0 d\log(D_p) \quad (4)$$

As such, the fine particle mass concentration ($PM_{2.5}$) can be calculated by integrating the normalized particle mass size distribution up to 2.5 μm :

$$PM_{2.5} = \int_{0.01}^{2.5} n_M^0 d\log(D_p) \quad (5)$$

The submicron particle number concentration can be calculated by integrating the normalized particle number size distribution up to 1 μm

$$PN_1 = \int_{0.01}^1 n_N^0 d\log(D_p) \quad (6)$$

2.4. Weather Conditions

For this study's analysis, we included only temperature and relative humidity data collected from April 10 to April 28, 2022.

April, being part of the spring season, generally has moderate temperatures and variable relative humidity. These conditions guarantee accurate readings and do not lead to the failure of the devices, as high temperatures are not suitable for these devices. Sometimes, dust storms may occur during this season in several regions of Jordan, especially the eastern and southern regions. During all measurement campaigns, relative humidity mostly ranged from 12% to 55%, and temperatures varied between 12°C and 32°C, with a median of 22°C.

3. Results and Discussion

3.1. Particle Number Concentrations

3.1.1. Submicron Particle Number (PN_1) Concentrations

The mid-western region of Jordan was the main focus of this study. The spatial variation of PN_1 is shown in Fig. 2 and listed in Table 1. This data suggests that traffic emissions are the main reasons for high aerosol concentrations in Jordan. The measurements were taken in more than 20 sites within Karak. Most of these sites did not have intensive traffic activity. As discussed in this and the next subsections, the particle number size distribution also reflects the spatial variation in concentrations (Fig. 3).

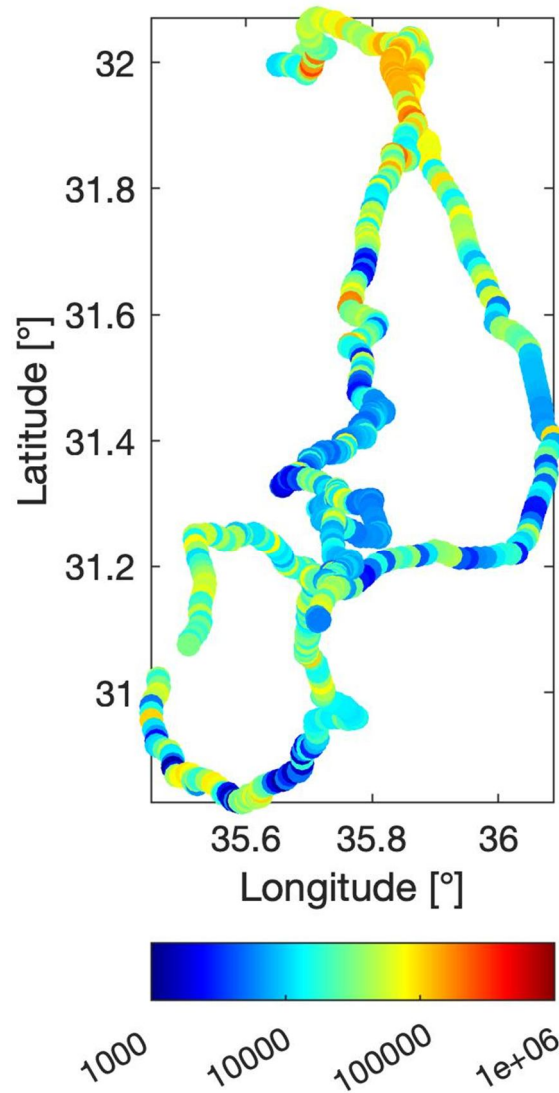


FIG. 2. Total particle number concentrations (PN_1) plotted on the measurement routes.

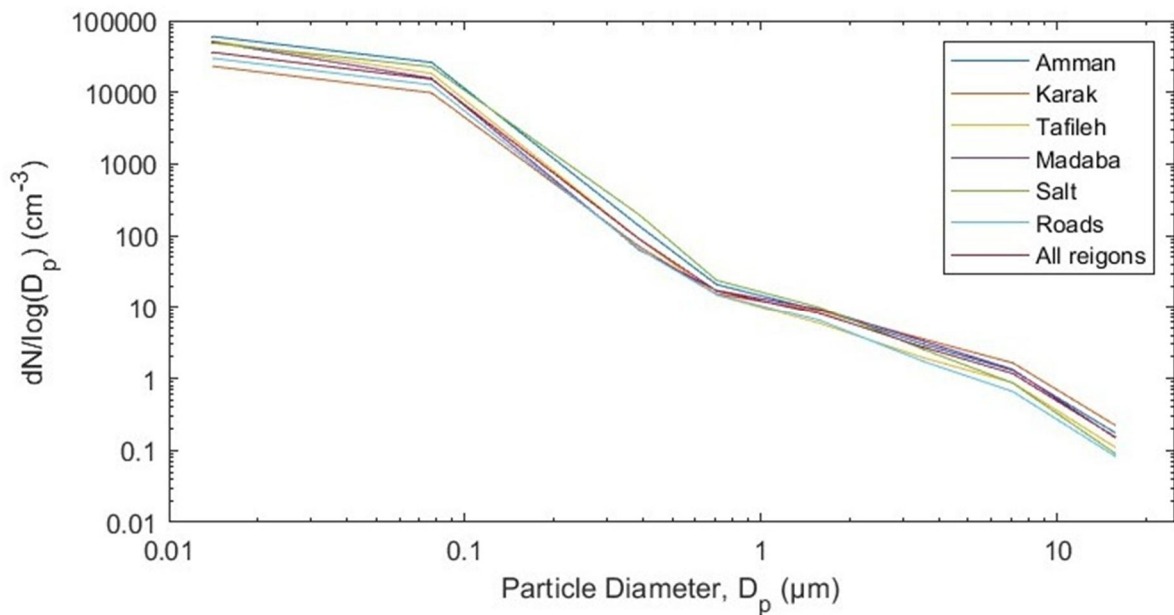


FIG. 3. Average particle number size distributions (n_N^0) derived from the merge of the three instruments: CPC, P-Trak, and AeroTrak.

TABLE 1. Average submicron particle number concentrations (PN_1 [cm^{-3}]).

	Size fraction	mean	Std.	min	5%	25%	Median	75%	95%	max	#
Cities	Amman	46000	42400	7500	8100	16300	31900	56300	131900	243700	284
	Salt	43900	49300	10600	11000	13300	32400	45700	147000	287600	74
	Madaba	37000	38000	2200	2900	11800	30500	47300	99400	184800	52
	Karak	19700	18400	1500	4500	7700	11000	27000	58900	134400	430
	Tafila	40500	25900	1100	2400	26700	36300	55100	90000	110100	31
Roads	Amman-Salt	66400	33100	34500	35900	41700	54500	84600	120200	137000	10
	Amman-Madaba	39000	29200	9100	12200	14100	34200	47500	80500	132600	21
	Madaba-Karak	6400	3600	2500	2600	3700	5500	7500	14400	17500	45
	Amman-Karak (Desert)	30600	30700	2600	4400	8700	16700	43200	89600	166800	71
	Qatrana-Karak	15800	13700	2400	2800	4400	11500	28200	37700	45200	21
	Karak-Dead sea	21300	17700	7900	8300	10400	14300	27100	52700	115200	74
	Dead sea industry	29100	20300	2400	8400	13700	22400	40400	63100	101100	50
	Dead sea-Tafila	31500	28600	1200	1500	6500	23800	46300	81700	91400	27
	Tafila-Karak	15500	11600	1200	1800	12200	13400	17600	38300	73000	65

TABLE 2. Average micron particle number concentrations (PN_{10-1} [cm^{-3}]).

	Size fraction	mean	Std.	min	5%	25%	Median	75%	95%	max	#
Cities	Amman	5	3	2	2	3	4	6	9	18	284
	Salt	5	1	3	3	4	5	5	7	9	74
	Madaba	5	2	3	4	4	5	6	7	13	52
	Karak	5	3	2	3	4	5	6	9	31	430
	Tafila	3	1	2	2	3	3	3	7	8	31
Roads	Amman-Salt	4	1	3	3	4	4	4	5	5	10
	Amman-Madaba	5	1	4	4	5	5	5	7	8	21
	Madaba-Karak	5	1	2	2	4	5	5	8	9	45
	Amman-Karak (Desert)	2	1	2	2	2	2	3	5	9	71
	Qatrana-Karak	2	0	2	2	2	2	2	4	4	21
	Karak-Dead sea	2	0	2	2	2	2	2	4	6	74
	Dead sea industry	4	7	2	2	2	2	2	7	52	50
	Dead sea-Tafila	2	0	2	2	2	2	2	2	5	27
	Tafila-Karak	2	1	2	2	2	2	2	5	6	65

The PN_1 was the lowest in Karak ($\sim 1.97 \times 10^4 \text{ cm}^{-3}$) among the regions studied. For example, it was $\sim 4.6 \times 10^4 \text{ cm}^{-3}$ in Amman and $\sim 4.4 \times 10^4 \text{ cm}^{-3}$ in Salt. These were the highest throughout this study. In Madaba it was $\sim 3.7 \times 10^4 \text{ cm}^{-3}$ (measured during 10:00–11:30 on April 28) and $\sim 3.7 \times 10^4 \text{ cm}^{-3}$ in Tafila (measured during 14:00–15:30 on April 12). Although Madaba and Tafila are small towns in Jordan, the relatively high PN_1 levels can be attributed to the measurements taken on the main roads with high traffic activities and related emissions (Table 1).

As for the main roads connecting cities, the overall average PN_1 was $\sim 2.3 \times 10^4 \text{ cm}^{-3}$. The concentration was the highest on the road between Amman and Salt ($\sim 6.6 \times 10^4 \text{ cm}^{-3}$). The lowest concentrations were observed along the main roads connecting Karak and Madaba (less than 10^4 cm^{-3}). For instance, the PN_1 in the Dhiban area was about half of that reported in Madaba. On the desert road between Amman and Karak, the mean concentration was about $4 \times 10^4 \text{ cm}^{-3}$. This road had active traffic of heavy-duty vehicles (e.g. trucks and lorries). As the traffic activity was low on the road between Al-Qatraneh and Karak, the concentration was considerably low (about $1.6 \times 10^4 \text{ cm}^{-3}$), similar to the Tafila–Karak road, which winds through mountainous terrain near Al-Tanour Dam and resembles the conditions on the Madaba–Karak route through Dhiban. On the road passing by the southern part of the Dead Sea, the concentration was about $3 \times 10^4 \text{ cm}^{-3}$ (Table 1).

It is worth mentioning that the measurements were taken in Amman on different dates (April 10, 12, and 28) at various times and locations: Jubaiha, Sweileh, part of the airport road, Marj Al-Hamam, and Naour. All these measurements were taken during the morning period. This variability suggests that PN_1 concentrations in Amman can fluctuate significantly. For further context, Hussein *et al.* reported that PN_1 concentrations at an urban background location (University of Jordan campus) ranged between 15000 cm^{-3} and 40000 cm^{-3} [12]. Additionally, these results can be compared to the results of a study conducted in Amman in 2014, where the mean PN_1 concentration was $11 \times 10^4 \text{ cm}^{-3}$. The reason for this increase is that the measurements were taken in many areas of Amman and included peak times.

3.1.2. Micron Particle Number (PN_{10-1}) Concentrations

The PN_{10-1} varied considerably from one location to another. The highest concentration was about 5 cm^{-3} , recorded in Amman, Salt, Madaba, and Karak. Interestingly, the concentration in Tafila was about 3 cm^{-3} (Table 2). The high concentrations of micron particles in these cities can be partly due to road dust re-suspension.

The overall average PN_{10-1} on the main roads was about 3 cm^{-3} and it varied between 2 cm^{-3} and 5 cm^{-3} . The highest concentration ($\sim 5 \text{ cm}^{-3}$) was observed on the road from Amman to Karak passing through Madaba. Concentrations on the Amman–Salt road and near the Dead Sea were about 4 cm^{-3} . The rest of the tested roads had a PN_{10-1} concentration of about 2 cm^{-3} .

Interestingly, the PN_{10-1} concentrations were more variable on roads than within cities. It can be due to the fact that on some roads traffic activity was not as high as on other roads. In cities, traffic activity remains relatively high throughout the day, and the road dust dispersed within the city reaches a rather steady-state concentration, which was considerably high ($\sim 5 \text{ cm}^{-3}$).

3.2. Particulate Matter (PM) Concentrations

3.2.1. Micron and Super Micron Particulate Matter ($PM_{10-2.5}$ and PM_{25-10})

Amman had the lowest PM_{10-1} concentrations, which was $\sim 22 \mu\text{g m}^{-3}$ (Table 3). This is because the studied areas in Amman (University of Jordan, Jubaiha, Marj Al-Hamam) are devoid of quarries and farms. The PM_{25-10} concentrations in Amman were about ($\sim 141 \mu\text{g m}^{-3}$). This indicates that Amman is also clearly affected by sand and dust storm (SDS) episodes coming from the eastern and southern regions.

The mean concentration of PM_{10-1} increased to $\sim 74 \mu\text{g m}^{-3}$ when we moved westward to the city of Salt, while the PM_{25-10} concentrations decreased to $\sim 73 \mu\text{g m}^{-3}$, reflecting Salt's distance from desert regions and reduced local dust storm impact.

The PM_{10-1} and PM_{25-10} concentrations in Madaba were $105 \mu\text{g m}^{-3}$ and $120 \mu\text{g m}^{-3}$, respectively. The concentration of PM_{10-1} in the city center was high and then decreased when we moved south to Theban, whereas PM_{25-10} followed an opposite trend, confirming what we

discussed previously. Tafila showed a similar pattern, with the average concentration of PM_{10-1} and PM_{25-10} of $67 \mu\text{g m}^{-3}$ and $89 \mu\text{g m}^{-3}$, respectively.

Karak had the highest PM_{10-1} and PM_{25-10} concentrations ($\sim 123 \mu\text{g m}^{-3}$ and $\sim 180 \mu\text{g m}^{-3}$, respectively), due to the large spread of quarries, crushers, and farms in the non-urban areas along the measurement path in addition to the effect of dust storms coming from the desert areas east of Karak.

The mean PM_{10-1} and PM_{25-10} concentrations on the Amman-Madaba road were high ($\sim 112 \mu\text{g m}^{-3}$ and $107 \mu\text{g m}^{-3}$, respectively). This increase in the average PM_{10-1} and PM_{25-10} concentrations may be due to the presence of many farms west of the road (Table 4). This is repeated on the Jordan Valley road that borders the Dead Sea from the Ghor Al Mazraa to the Ghor Al Fifa, where the average PM_{10-1} and PM_{25-10} concentrations are also high ($84 \mu\text{g m}^{-3}$ and $143 \mu\text{g m}^{-3}$, respectively). In this area, there are also a large number of farms and some factories. This leads us to conclude that the average concentrations of PM_{10-1} and PM_{25-10} are

high on roads with significant agricultural activities, and the average concentration is low on roads free of farms.

The particle mass size distribution can be best represented by eight particle size fractions: 10–25 nm, 25–300 nm, 0.3–0.5 μm , 0.5–2.5 μm , 2.5–5 μm , 5–10 μm , and 10–25 μm . The particle mass size distribution shows that the high concentrations in all regions of the 10–25 μm particle size-fraction is caused by dust (Fig. 4).

3.2.2. Submicron and Fine Particulate Matter

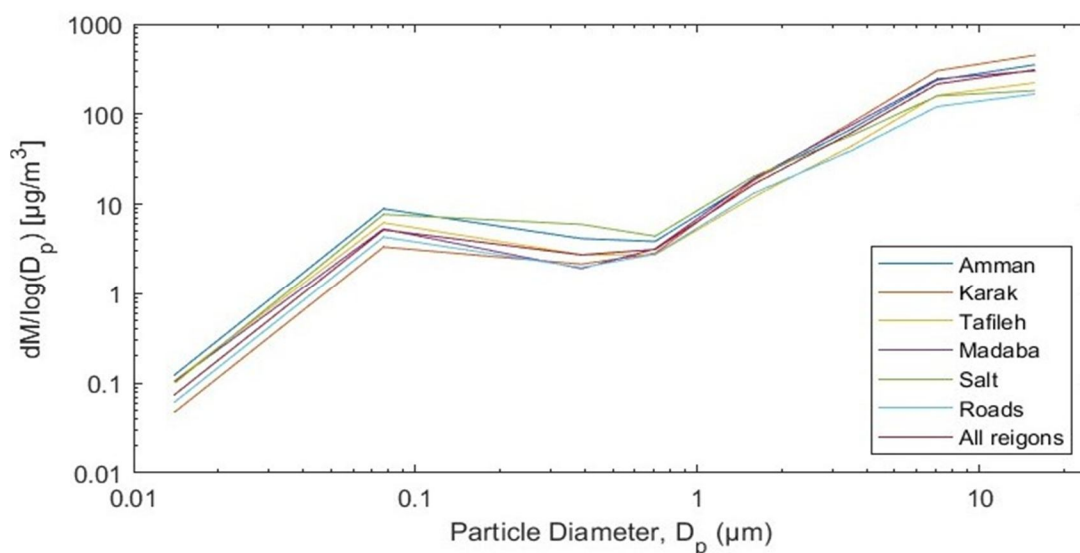
$PM_{1-0.3}$ concentrations were higher across the cities than on the main roads, except for Karak, where the $PM_{1-0.3}$ concentrations were the lowest ($\sim 5 \mu\text{g m}^{-3}$), likely due to dilution from clean air in that area. Amman and Salt had the highest concentrations ($\sim 12 \mu\text{g m}^{-3}$ and $\sim 11 \mu\text{g m}^{-3}$, respectively), which can be attributed to higher traffic activity compared to other study areas. In Madaba and Tafila, $PM_{1-0.3}$ concentrations were $\sim 7 \mu\text{g m}^{-3}$ and $\sim 8 \mu\text{g m}^{-3}$, respectively, and these concentrations decreased when we moved away from the main streets in the city centers in both regions (Table 3).

TABLE 3. Average particulate matter concentrations ($\mu\text{g}/\text{m}^3$) in different size fractions measured across the cities.

	Size fraction	mean	Std.	min	5%	25%	Median	75%	95%	max	#
Amman	$PM_{1-0.3}$	12	11	2	3	6	7	15	56	72	284
	PM_{10-1}	22	94	17	34	54	71	127	203	887	284
	PM_{25-10}	141	264	23	32	64	95	142	275	3000	284
Karak	$PM_{1-0.3}$	5	4	1	2	2	3	7	20	37	430
	PM_{10-1}	123	121	26	39	64	93	135	288	1200	430
	PM_{25-10}	180	265	8	36	68	104	190	488	2600	430
Madaba	$PM_{1-0.3}$	7	6	1	2	3	6	10	30	29	52
	PM_{10-1}	105	46	61	66	80	94	116	161	309	52
	PM_{25-10}	120	90	53	64	77	96	138	207	650	52
Tafila	$PM_{1-0.3}$	8	5	1	1	5	7	11	26	22	31
	PM_{10-1}	67	73	24	30	37	40	55	252	313	31
	PM_{25-10}	89	120	14	22	40	48	77	393	507	31
Salt	$PM_{1-0.3}$	11	11	4	4	5	9	11	45	68	74
	PM_{10-1}	74	44	39	43	52	60	75	151	282	74
	PM_{25-10}	73	79	19	29	40	52	70	185	544	74
All roads	$PM_{1-0.3}$	6	6	1	1	3	4	7	25	53	394
	PM_{10-1}	53	111	15	18	26	36	58	121	2100	394
	PM_{25-10}	67	249	6	11	21	35	61	149	4700	394
All regions	$PM_{1-0.3}$	7	8	1	1	3	5	8	32	80	1265
	PM_{10-1}	89	108	14	22	40	63	102	215	2100	1265
	PM_{25-10}	122	244	6	16	39	72	121	336	4700	1265

TABLE 4. Average particulate matter ($\mu\text{g}/\text{m}^3$) in different size fractions measured on main roads.

	Size fraction	mean	Std.	min	5%	25%	Median	75%	95%	max	#
Amman-Salt	PM _{1-0.3}	14	5	9	9	9	12	17	40	26	10
	PM ₁₀₋₁	62	8	51	51	56	61	66	73	75	10
	PM ₂₅₋₁₀	53	11	39	39	44	52	62	69	72	10
Amman-Madaba	PM _{1-0.3}	9	5	2	3	5	5	9	32	21	21
	PM ₁₀₋₁	112	21	82	83	98	108	120	142	159	21
	PM ₂₅₋₁₀	107	31	70	76	87	99	117	159	193	21
Madaba-Karak	PM _{1-0.3}	2	1	2	2	2	2	2	5	5	45
	PM ₁₀₋₁	64	24	42	44	53	59	70	96	190	45
	PM ₂₅₋₁₀	80	72	24	35	45	58	83	206	443	45
Amman-Karak (Desert)	PM _{1-0.3}	8	7	2	2	3	5	10	36	41	71
	PM ₁₀₋₁	38	25	16	19	24	30	39	84	179	71
	PM ₂₅₋₁₀	34	31	7	9	17	23	36	102	182	71
Qatrana-Karak	PM _{1-0.3}	4	3	2	2	2	3	5	15	12	21
	PM ₁₀₋₁	31	14	16	17	21	26	38	59	68	21
	PM ₂₅₋₁₀	31	45	7	8	13	16	28	75	215	21
Karak-Dead sea	PM _{1-0.3}	6	5	2	2	3	4	5	22	38	74
	PM ₁₀₋₁	37	19	21	22	26	33	40	57	134	74
	PM ₂₅₋₁₀	37	27	9	13	21	31	42	85	182	74
Dead sea industry	PM _{1-0.3}	6	4	1	2	4	6	8	20	21	50
	PM ₁₀₋₁	84	291	17	22	27	32	42	151	2077	50
	PM ₂₅₋₁₀	143	666	11	16	24	32	47	204	4743	50
Dead sea-Tafila	PM _{1-0.3}	5	0	4	4	4	5	5	14	6	27
	PM ₁₀₋₁	53	83	17	20	25	28	41	109	449	27
	PM ₂₅₋₁₀	30	60	6	7	11	13	21	63	319	27
Tafila-Karak	PM _{1-0.3}	4	2	1	1	4	4	5	12	13	65
	PM ₁₀₋₁	55	55	18	22	28	40	57	191	291	65
	PM ₂₅₋₁₀	84	116	7	14	27	47	95	306	670	65


 FIG. 4. Average particle mass size distributions (n_M^0) derived across cities and along main roads.

On the main roads, the highest average concentration was observed on the Amman-Salt Road ($\sim 15 \mu\text{g m}^{-3}$), which connects two urban

areas close to each other. Then there is the Amman-Madaba road and the Desert Road ($\sim 9 \mu\text{g m}^{-3}$), which are sometimes exposed to dust

storms that occur during this period of the year. As for the lowest average concentration, it was on the Karak-Madaba road ($\sim 2 \mu\text{g m}^{-3}$). On other roads, the average $\text{PM}_{1-0.01}$ concentrations ranged between ($5 \mu\text{g m}^{-3}$ and $7 \mu\text{g m}^{-3}$).

The average $\text{PM}_{2.5}$ concentration within Amman, especially near the University of Jordan and the areas around it, was about $19 \mu\text{g m}^{-3}$ (Table 5) This average increased as we went to the southwest side, where the average $\text{PM}_{2.5}$ concentration was $21 \mu\text{g m}^{-3}$ in Marj Al-Hamam, and $34 \mu\text{g m}^{-3}$ in Naour, likely due to nearby small industrial complexes and the movement of heavy machinery. This concentration did not decrease when we headed west to Salt ($19 \mu\text{g m}^{-3}$). In Madaba, the concentration was $15 \mu\text{g m}^{-3}$. We observed that the concentration of $\text{PM}_{2.5}$ in the city center was high and then decreased when we moved south to Theban. The average concentrations continued to decrease as

we moved south to Karak and Tafila ($12 \mu\text{g m}^{-3}$ and $13 \mu\text{g m}^{-3}$, respectively).

On the main roads, the highest concentrations were on the Amman-Salt road and the Amman-Madaba road ($22 \mu\text{g m}^{-3}$ and $17 \mu\text{g m}^{-3}$, respectively). The lowest concentrations ($8 \mu\text{g m}^{-3}$) were recorded on the road between Madaba and Karak, the Tafila-Karak road, and on the road between Ghor and Tafila, likely due to similar mountainous geography. The average concentrations on the road between Amman and Karak and the Dead Sea Road (industrial areas) were $13 \mu\text{g m}^{-3}$. The reason for the increase in the average concentration is the presence of industrial complexes situated along these routes.

Comparison of $\text{PM}_{2.5}$ and PN_1 concentrations indicated a positive linear relationship (Fig. 5), suggesting that emissions of both $\text{PM}_{2.5}$ and PN_1 likely originate from similar sources.

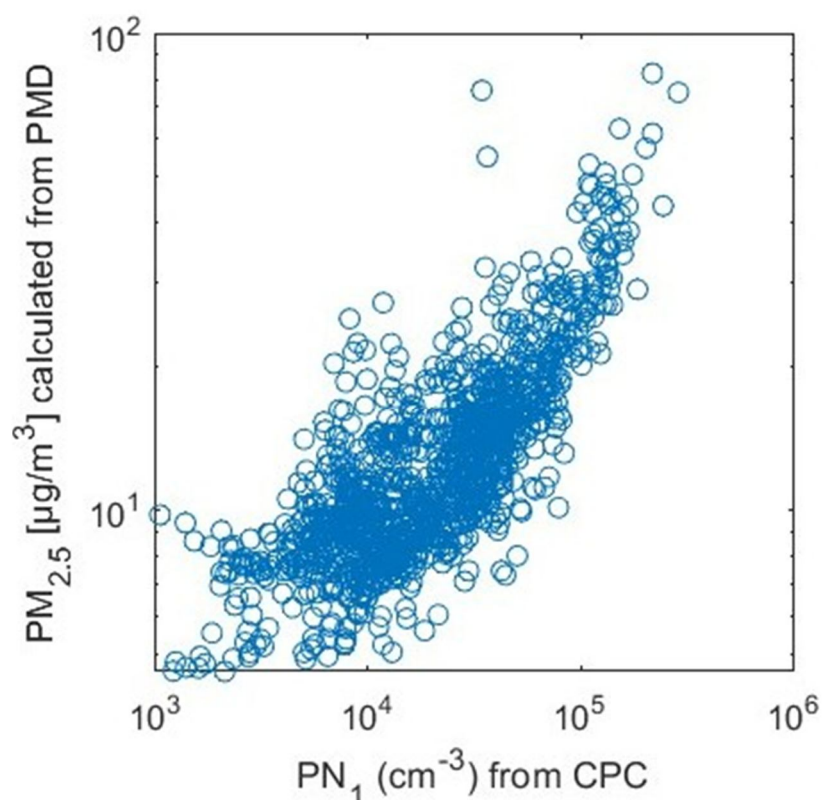


FIG. 5. A comparison between the PN_1 concentrations and calculated $\text{PM}_{2.5}$ concentrations.

Additionally, $PM_{2.5}$ concentrations were measured using the LCS device. The use of LCS devices in making measurements is a good addition to the study. In fact, three low-cost sensitive devices were used, and then the results of the three devices were averaged. This leads to more accurate results, as it was found that there is a variation in the levels of $PM_{2.5}$ concentrations from one region to another (Fig. 6). The average $PM_{2.5}$ concentrations measured with the LCS in Amman and Salt ranged between $11 \mu\text{g m}^{-3}$ and $13 \mu\text{g m}^{-3}$, while in Karak and Madaba they ranged between $12 \mu\text{g m}^{-3}$ and $14 \mu\text{g m}^{-3}$. The lowest concentration was in Tafilah ($\sim 7 \mu\text{g m}^{-3}$). On the main roads, the highest average concentration was on the Madaba-Karak road and the lowest

on the Tafilah-Karak road. This is largely consistent with the results of PMD.

Comparing the $PM_{2.5}$ concentrations calculated from the PMD with the $PM_{2.5}$ concentrations that were measured by the LCS devices in all regions included in the study showed a positive linear relationship (Fig. 7). In some areas, such as Karak, Madaba, and many areas within the governorates, and on some main and secondary roads, there was a match or convergence in the $PM_{2.5}$ concentrations measured by the LCS devices and the $PM_{2.5}$ concentrations calculated from the PMD. This means that the LCS devices can be relied upon to measure the $PM_{2.5}$ concentrations with the same efficiency as the AeroTrak device.

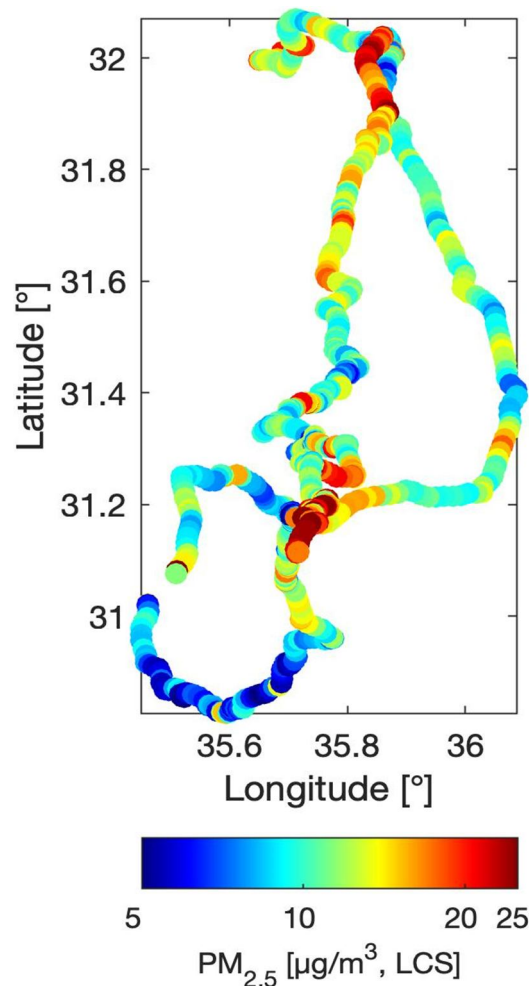


FIG. 6. Fine particulate matter ($PM_{2.5}$) concentrations plotted on the measurement routes.

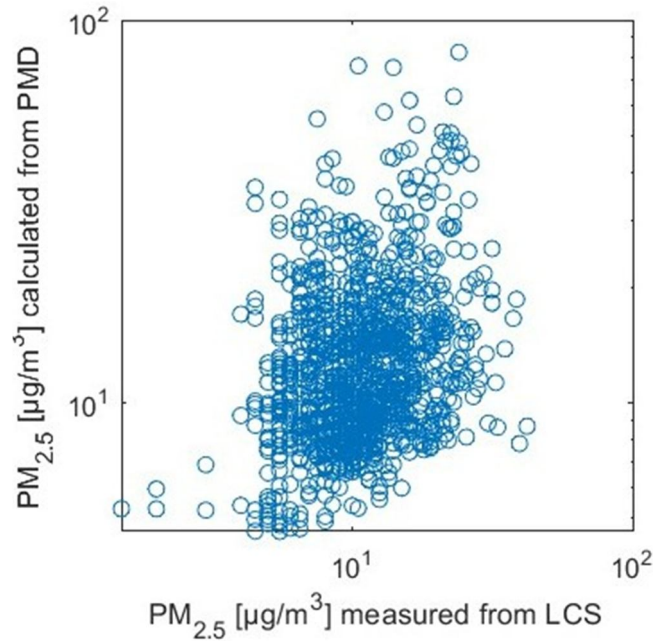


FIG. 7. A comparison between the $PM_{2.5}$ concentrations measured by the low-cost sensors (LCS) and calculated $PM_{2.5}$ concentrations.

TABLE 5. Average $PM_{2.5}$ concentrations measured by the LCS device compared to the calculated $PM_{2.5}$ concentrations (here marked as PMD).

	Location		mean	Std.	min	5%	25%	Median	75%	95%	max	#
Cities	Amman	LCS	11	6	2	5	6	9	17	23	27	284
		PMD	19	12	5	8	11	15	22	45	82	284
	Karak	LCS	13	6	5	6	9	12	16	26	39	430
		PMD	12	5	7	8	9	11	14	21	55	430
	Madaba	LCS	14	3	10	10	12	13	16	19	22	52
		PMD	15	7	8	8	10	14	17	28	39	52
	Tafila	LCS	7	3	5	5	6	6	7	14	17	31
		PMD	13	5	5	7	10	12	16	20	25	31
	Salt	LCS	13	3	8	10	12	13	15	19	20	74
		PMD	19	10	13	14	14	15	20	35	75	74
Amman-Salt	LCS	11	1	10	10	10	11	11	12	13	10	
	PMD	21	5	16	16	17	19	25	28	29	10	
Amman-Madaba	LCS	15	1	13	14	14	15	16	17	17	21	
	PMD	17	5	10	11	14	15	21	26	27	21	
Madaba-Karak	LCS	10	2	7	8	9	10	12	13	14	71	
	PMD	13	7	5	7	8	11	16	29	43	71	
R(Desert)	LCS	12	2	9	10	11	12	14	15	15	21	
	PMD	9	3	5	6	6	8	10	14	15	21	
Roads	Qatrana-Karak	LCS	12	3	7	8	9	11	14	18	19	45
		PMD	8	1	7	7	7	8	8	10	11	45
Karak-Dead sea	LCS	9	2	6	7	8	9	10	12	15	74	
	PMD	10	5	6	7	7	9	11	21	37	74	
Dead sea industry	LCS	12	7	5	6	9	10	12	24	42	49	
	PMD	13	10	5	6	8	11	15	20	76	50	
Dead sea- Tafila	LCS	6	1	5	5	5	6	6	8	9	26	
	PMD	8	4	5	5	5	7	9	16	21	27	
Tafila-Karak	LCS	8	3	5	5	7	8	10	15	18	65	
	PMD	8	2	5	5	7	8	9	13	17	65	

4. Conclusion

We evaluated aerosol concentrations (including particle number, mass, and size distribution) in northwestern Jordan (Amman, Salt, Madaba, Tafila, and Karak) using a simple mobile setup during April 2022.

The submicron particle number (PN_1) concentration was highest in Amman ($4.6 \times 10^4 \text{ cm}^{-3}$), followed by Salt ($4.4 \times 10^4 \text{ cm}^{-3}$), Karak ($2.0 \times 10^4 \text{ cm}^{-3}$), and Tafila ($4.1 \times 10^4 \text{ cm}^{-3}$). On the main roads, the highest PN_1 was on Amman-Salt road ($6.6 \times 10^4 \text{ cm}^{-3}$), followed by the road between Amman and Salt ($3.9 \times 10^3 \text{ cm}^{-3}$). The lowest PN_1 ($6.4 \times 10^3 \text{ cm}^{-3}$) was observed on the road between Madaba and Karak via Dhiban. On other roads considered in this study, the concentrations varied between $1.5 \times 10^4 \text{ cm}^{-3}$ and $3.1 \times 10^4 \text{ cm}^{-3}$. The mean micron particle number (PM_{10-1}) concentrations varied between 2 and 5 cm^{-3} on roads and 3–5 cm^{-3} in cities.

Similar to the PN concentrations findings, the micron particulate mass (PM_{10-1}) concentrations were higher across the cities than on main roads, except for the road between Amman and Madaba. Karak and Madaba had the highest PM_{10-1} concentrations of $\sim 128 \mu\text{g m}^{-3}$ and $\sim 112 \mu\text{g m}^{-3}$, respectively, whereas Amman had the lowest PM_{10-1} concentrations of $\sim 34 \mu\text{g m}^{-3}$. The concentrations on the road between Amman and Madaba (mean value $\sim 120 \mu\text{g m}^{-3}$), were the highest, whereas the main road from Amman through Qatrana towards Karak had the lowest PM_{10-1} concentrations (lower than $32 \mu\text{g m}^{-3}$).

Karak had the highest PM_{10-25} concentrations ($\sim 180 \mu\text{g m}^{-3}$), whereas Salt had the lowest PM_{10-25} concentrations ($\sim 73 \mu\text{g m}^{-3}$). Concentrations were also high along the Jordan Valley road ($\sim 143 \mu\text{g m}^{-3}$), but low on the main road from Amman through Qatrana towards Karak and the road between Al-Ghor and Al-Tafila (lower than $34 \mu\text{g m}^{-3}$).

The average concentrations of $PM_{2.5}$ decreased as we moved southward from Amman.

It was found that the topography and geographical nature, as well as the presence of industrial clusters, have a clear effect on the difference in concentrations from one region to another.

The PN and PM concentrations observed in this study suggest that traffic emissions are the main sources of aerosols in cities. The southernmost locations (i.e. Karak) were mainly affected by dust aerosols due to local sand re-suspension from desert areas.

This study's primary limitation is the short measurement duration. Further research is needed to improve understanding of the air pollution in Jordan. Currently, there is a lack of information about aerosol temporal and spatial variations, the impact of aerosols on weather and vice versa, and trends in dust outbreaks. Such information can be gathered via long-term measurements as well as extensive short-term measurement campaigns. Measurements of the particle size distribution are also needed to understand the dynamic behavior of particulate matter. Furthermore, physical and chemical characterizations are highly needed to better understand the toxicity and health effects, as well as the formation and transformation processes of air pollution.

For future research, we strongly recommend conducting long-term aerosol measurements at several sites throughout the country, complemented by extensive and repeated mobile measurement campaigns.

Acknowledgments

This study was supported by the Deanship of Scientific Research (DSR) at the University of Jordan. This work was conducted as part of a close collaboration between the University of Jordan and the Institute for Atmospheric and Earth System Research (INAR) at the University of Helsinki.

References

- [1] Lohmann, U. and Feichter, J., *Atmos. Chem. Phys.*, 5 (2005) 715.
- [2] Boman, J., Shaltout, A. A., Abozied, A. M., and Hassan, S. K., *X-Ray Spectrom.*, 42 (2013) 276.
- [3] Rushdi, A. I., Al-Mutlaq, K. F., Al-Otaibi, M., El-Mubarak, A. H., and Simoneit, B. R. T., *Arabian J. Geosci.*, 6 (2013) 585.
- [4] Dada, L., Mrad, R., Siffert, S., and Saliba, N.A., *J. Aerosol. Sci.*, 66 (2013) 187.

- [5] Alam, K., Mukhtar, A., Shahid, I., Blaschke, T., Majid, H., Rahman, S., Khan, R., and Rahman, N., *Aerosol. Air Qual. Res.*, 14 (2014) 1851.
- [6] Alam, K., Trautmann, T., Blaschke, T., and Subhan, F., *Remote Sens. Environ.*, 143 (2014) 216.
- [7] Gherboudj, I. and Ghedira, H., *Int. J. Climatol.*, 34 (2014) 3321.
- [8] Hussein, T., Al-Ruz, R. A., Petäjä, T., Junninen, H., Arafah, D.-E., Hämeri, K., and Kulmala, M., *Aerosol. Air Qual. Res.*, 11 (2011) 109.
- [9] Hussein, T., Boor, B. E., dos Santos, V. N., Kangasluoma, J., Petäjä, T., and Lihavainen, H., *Aerosol. Air Qual. Res.*, 17 (2017) 1875.
- [10] Hussein, T. and Betar, A., *Jordan J. Phys.*, 10 (2017) 51.
- [11] Hussein, T., Dada, L., Hakala, S., Petäjä, T., and Kulmala, M., *Atmosphere*, 10 (2019) 710.
- [12] Hussein, T., Saleh, S. S. A., dos Santos, V. N., Abdullah, H., and Boor, B.E., *Atmosphere*, 10 (2019) 323.
- [13] Hussein, T., Halayaka, M., Al-Ruz, R. A., Abdullah, H., Mølgaard, B., and Petäjä, T., *Jordan J. Phys.*, 9 (2016) 31.
- [14] Basha, G., Phanikumar, D. V., Kumar, K. N., Ouarda, T. B. M. J., and Marpu, P. R., *Remote Sens. Environ.*, 169 (2015) 404.
- [15] Saliba, N. A., Kouyoumdjian, H., and Roumié, M., *Atmos. Environ.*, 41 (2007) 6497.
- [16] Roumie, M., Chiari, M., Srour, A., Sa'adeh, H., Reslan, A., Sultan, M., Ahmad, M., Calzolari, G., Nava, S., Zubaidi, Th., Rihawy, M. S., Hussein, T., Arafah, D.-E., Karydas, A. G., Simon, A., and Nsouli, B., *Nucl. Instrum. Methods Phys. Res. B*, 371 (2016) 381.
- [17] Tadros, M. T. Y., Madkour, M., and Elmetwally, M., *Renew. Energy*, 174 (1999) 339.
- [18] Moustafa, M., Mohamed, A., Ahmed, A.-R., and Nazmy, H., *J. Adv. Res.*, 6 (2014) 827.
- [19] Hussein, T., Juwhari, H., Al Kuisi, M., Alkattan, H., Lahlouh, B., and Al-Hunaiti, A., *Arabian J. Geosci.*, 11 (2018) 617.
- [20] Hussein, T., Li, X., Al-Dulaimi, Q., Daour, S., Atashi, N., Viana, M., Alastuey, A., Sogacheva, L., Arar, S., Al-Hunaiti, A., and Petäjä, T., *Aerosol. Air Qual. Res.*, 20 (2020) 2780.
- [21] Hussein, T., Atashi, N., Sogacheva, L., Hakala, S., Dada, L., Petäjä, T., and Kulmala, M., *Atmosphere*, 11 (2020) 79.
- [22] Hussein, T., Li, X., Bakri, Z., Alastuey, A., Arar, S., Al-Hunaiti, A., Viana, M., and Petäjä, T., *Atmosphere*, 13 (2022) 197.
- [23] Al-Momani, I. F., Daradkeh, A. S., Haj-Hussein, A. T., Yousef, Y. A., Jaradat, Q. M., and Momani, K.A., *Atmos. Res.*, 73 (2005) 87.
- [24] Jiries, A., *Environmentalist*, 23 (2003) 205.
- [25] von Schneidemesser, E., Zhou, J., Stone, E. A., Schauer, J. J., Qasrawi, R., Abdeen, Z., Shpund, J., Vanger, A., Sharf, G., Moise, T., Brenner, S., Nassar, K., Saleh, R., Al-Mahasneh, Q. M., and Sarnat, J.A., *Atmos. Environ.*, 44 (2010) 3669.
- [26] Abdeen, Z., Qasrawi, R., Heo, J., Wu, B., Shpund, J., Vanger, A., Sharf, G., Moise, T., Brenner, S., Nassar, K., Sarnat, J. A., and Schauer, J. J., *Sci. World J.*, 2014 (2014) 78704.
- [27] Hussein, T., Puustinen, A., Aalto, P. P., Mäkelä, J. M., Hämeri, K. and Kulmala, M., *Atmos. Chem. Phys.*, 4 (2004) 391.